INTERFACIAL DELAMINATION AND MULTIPLE TUNNEL CRACKS TOUGHENING MECHANISMS OF LAMINATED TI-(TIBW) COMPOSITES UNDER THREE POINT BENDING TESTING

B.X. Liu[1, 2*], Lin Geng[3], LuJun Huang[3], XueWen Li[4], XiPing Cui[3], FuXing Yin[1, 2]

[1]Research Institute for Energy Equipment Materials, Hebei University of Technology, TianJin 300132, China; [2]TianJin key laboratory of materials laminating fabrication and interfacial controlling technology; [3]School of Materials Science and Engineering, Harbin Institute of Technology, Harbin 150001; [4]School of Materials Science and Engineering, Harbin University of Science and Technology, Harbin 150080, China; [*]Corresponding author email: liubaoxi@hebut.edu.cn

Keywords: Laminated composites, Interface voids, Tunnel crack, Delamination crack, Shear stress.

ABSTRACT

On the basis of idea that metal matrix composites with multi-scale hierarchical structures can obtain superior mechanical properties, a range of two-scale hierarchical laminated Ti-(TiBw/Ti) containing laminated and network structures were successfully fabricated by diffusion welding at different temperatures of 1000ºC, 1100ºC and 1200oC, respectively. This paper aims to clarify the influence rule of diffusion welding temperature, layer structure and interface on deformation behavior and fracture characteristics, and the deformation behavior, fracture mode and toughening mechanisms of the three laminated composites were investigated by three point bending testing in detail. Microstructure observation reveals that less interfacial voids and delamination phenomena are appeared with the increase of diffusion welding temperature. Laminated composites fabricated at 1000ºC exhibits a saw-tooth load displacement curve, the applied load sharply decreases in a manner of jagged style owing to the weak interface with super-low bonding strength, and fracture characteristics are characterized by serious interfacial delamination and less tunnel cracks compared to the other two laminated composites. The laminated Ti-(TiBw/Ti) composites fabricated at 1100ºC reveal the highest bending ductility and bending toughness, which is attributed to the moderate interfacial bonding strength. Bending fracture morphologies are characterized by many interfacial delamination cracks and multiple tunnel cracks, which can effectively toughened the laminated composites. On the basis of bending theory, the formation of multiple tunnel crack may be related to the high tensile strain and stress in the TiBw/Ti composite layer, while delamination crack may be initiated by shear stress. In addition, the laminated Ti-(TiBw/Ti) composites fabricated at 1200ºC displays sharply fracture stage when the load reaches to peak value, which is attributed to the strong interfacial bonding strength and absence of delamination cracks.

1 INTRODUCTION

Titanium matrix composites (TMCs) reinforced with ceramic fibers, whiskers or particles have drawn great attention due to their low density, heat resistance, promising special stiffness and special strength. However, TMCs usually exhibit low ductility and fracture toughness compared with monolithic titanium alloy with the addition of reinforcements, which seriously limits their application in aerospace and automotive industry [1-3]. Lu [4, 5] proposed an idea that the mechanical properties of composites can be enhanced by tailoring the distribution of reinforcements to form novel multi-scale structures, network [6], laminated [7] and gradient [8] distribution structure are the multi-scale hierarchical structures.

The improvement in fracture properties of laminated composites can be mainly attributed to two categories: intrinsic (particle spacing, grain size and particle spacing, etc) and extrinsic (residual stress, crack deflection, etc) toughening mechanisms. Laminated structural materials involve energy dissipative mechanisms to develop "flaw-tolerant" materials [9], so it is a useful approach to improve the mechanical behavior. Clegg [10] firstly reported a method of preparing toughening laminated ceramics by coating silicon carbide sheets with graphite based on the idea of nacre structure in nature,

which obviously reduce crack propagation velocity and improve the fracture toughness by introducing weak interfaces. Jiang [11] proposed a flake powder metallurgy method to prepare nano-laminated CNT/Al composites, which display well-balanced strength and ductility.

In our previous work [12-14], the tensile properties of two-scale laminated Ti-(TiBw/Ti) composites with different reinforcement volume fraction and layer thickness were investigated in detail, revealing high strength and superior fracture elongation under the unaxial tensile testing. In this paper, it is really interesting to further investigate the bending behaviors and fracture characteristics of the laminated Ti-(TiBw/Ti) composites by adjusting interfacial bonding status, which is useful to further comprehend the relationship between structure and performance and guide the microstructure design for property improvement of composites.

2 EXPERIMENTAL PROCEDURES

The laminated Ti-(TiBw/Ti) composites is comprised of Ti layer and TiBw/Ti composite layer, and the fabrication process of laminated composites were reported in our previous work [15], containing two sequence steps: the preparation of as-sintered 8vol. % composites with network microstructure and diffusion bonding method to fabricate laminated Ti-(TiBw/Ti) composites.

Firstly, the quantitative TiB_2 powders with fine size can be uniform adhered onto surface of titanium powders with large size by ball milled under pure Ar atmosphere. Then the mixture powders were taken into the graphite mold and hot pressed in vacuum (10^{-2}Pa) at 1200ºC under a pressure of 25MPa for 40min in order to obtain bulk TiBw/Ti composites with network microstructure. TiB phase is in situ synthesized according to the following reaction:

$$Ti+TiB_2 \rightarrow 2TiB \quad (1)$$

Based on the above reaction, 8vol. % composites with network reinforcement distribution were successfully fabricated. Then the as-sintered composites were cut into many sheets with different thickness by wire-cut machine. Meanwhile, the commercial pure Ti sheets were selected. In order to clean the oil and contaminant of the pure Ti and TiBw/Ti composite sheets, the thin sheets were corroded for two minutes in the 2vol. % HF solution and cleaned in water, then dried and alternatively stacked with Ti sheets in a graphite mold. Finally, the stacked composites were hot pressed in a vacuum atmosphere (10^{-2}) with a heating rate of 10ºC/min, and hold at 1000ºC, 1100ºC and 1200ºC under a pressure of 25MPa for 1h, the laminated Ti-(TiBw/Ti) composites were successfully fabricated by diffusion welding.

Microstructural examination was performed by optical microscopy (OM) and scanning electron microscopy (SEM, Hitachi S-4700) for the laminated composites after etching by 5%HF+15%HNO_3+85%H_2O solution. In order to provide a clear surface, the specimens were glued to a metallic platen and polished using a polishing machine. Bending specimens without notched crack have dimensions of 30 mm ×3 mm×4 mm and a total of five samples were tested for each mode. The bending testing process was carried out using an instron-5500 electronic universal test machine at room temperature in air with a crosshead speed of 0.5 mm/min.

3 RESULTS AND DISCUSSIONS

Fig. 1 shows the three laminated Ti-(TiBw/Ti) composites prepared by diffusion welding at different temperatures. It can be found that a ribbon region of interfacial macro-voids is presented in the laminated composite at the lowest temperature (1000ºC) as shown in the insert image of Fig. 1a), and the length of macro-void is about 50μm. As shown in the insert image of Fig. 1b), many interfacial micro-pores with size of 3~5μm are located in the laminated composites fabricated at 1100ºC. However, increasing the diffusion welding temperature up to 1200ºC, interfacial defects can be totally eliminated, forming a compact interface as shown in Fig. 1c). This result mainly ascribes to softening and thermal diffusion of Ti matrix at the interfacial region under the action of increasing temperature.

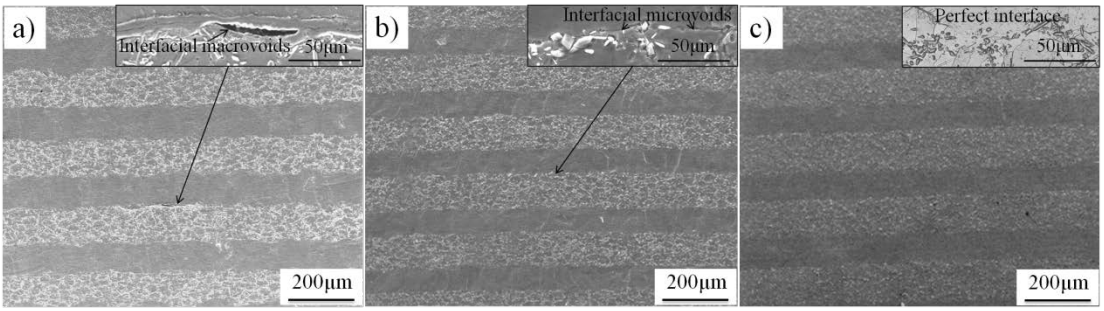

Fig. 1. The microstructures of laminated Ti-(TiBw/Ti) composites fabricated at different diffusion welding temperatures. a) 1000ºC; b) 1100ºC; c) 1200ºC.

In order to investigate the effect of diffusion welding temperature on mechanical properties, Fig. 2 shows the three-point bending load-deflection curves of laminated Ti-(TiBw/Ti) composites fabricated at 1000ºC, 1100ºC and 1200ºC, respectively. All the samples display a linear elastic stage and non-linear plastic deformation stage. However, laminated composite at 1000ºC reveals a saw-tooth load-displacement, which is different from those of laminated composites at 1100ºC and 1200ºC. The applied load decreases in a manner of jagged style, owing to the weak interface formed at low diffusion welding temperature of 1000ºC, and each top and root of saw-tooth corresponds to the delamination crack and crack propagation. Increasing the diffusion welding temperature to 1100ºC, the laminated composite reveals a prolong uniform plastic deformation process accompanying with non-catastrophic fracture stage. It is because that moderate interfaces can inhibit the propagation velocity of main crack propagation. However, when the diffusion welding temperature reaches to 1200ºC, laminated composites fracture rapidly after a peak load. Therefore, it is reasonable that the optimal diffusion welding temperature for three-point bending properties on mode I is 1100ºC, which exhibits an as-expected reasonable interfacial bonding strength.

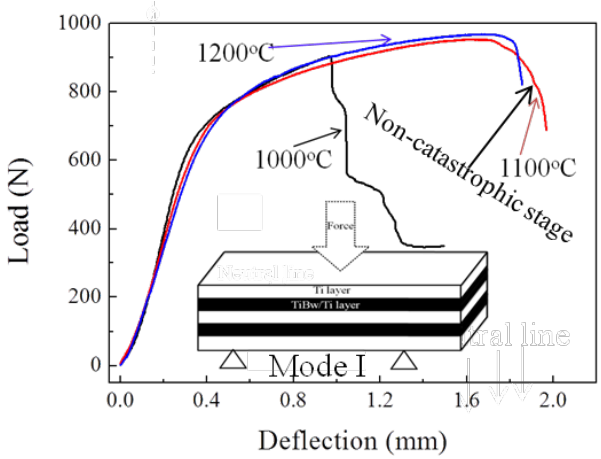

Fig. 2. The load-deflection curves of Ti-TiBw/Ti composites fabricated at different diffusion welding temperature.

Bending fracture characteristics of the laminated composite processed at 1100ºC show a complex fracture behavior as shown in Fig. 3. Fig. 3a) shows the macro fracture morphology corresponding to bending sample tested in crack arrester orientation (mode I), the main crack tortuous propagation path is accompanied with tunnel cracks and delamination cracks. The individual delamination crack presented in the interface, which may be due to that interfacial bonding strength is lower than bending shear stress. Otherwise, a single tunnel crack is existed in the TiBw/Ti composite layer as shown in Fig. 3b). The tunnel crack is attributed to the microcracks of fractured TiB whiskers, these micro-cracks grow and coalesce, and then reach macroscopic dimension with the increase of strain, which can result in fracture failure of TiBw/Ti composite layer. Fig. 3c) shows a mixture fracture characteristics of laminated Ti-(TiBw/Ti) composites: TiBw/Ti composite layers reveal tunnel crack initiated by nucleation, growth and coalescence of micro-cracks; while Ti layers reveal shear fracture with severe localized ductile damage, such as shear bands and localized necking. Moreover, obvious

localized plastic deformation traces and slight delamination cracks are appeared at the tunnel crack tip, which can effectively decrease stress concentration and propagation velocity of tunnel crack. Therefore, a prolong non-catastrophic fracture stage is existed in bending curves of laminated composites fabricated at 1100ºC.

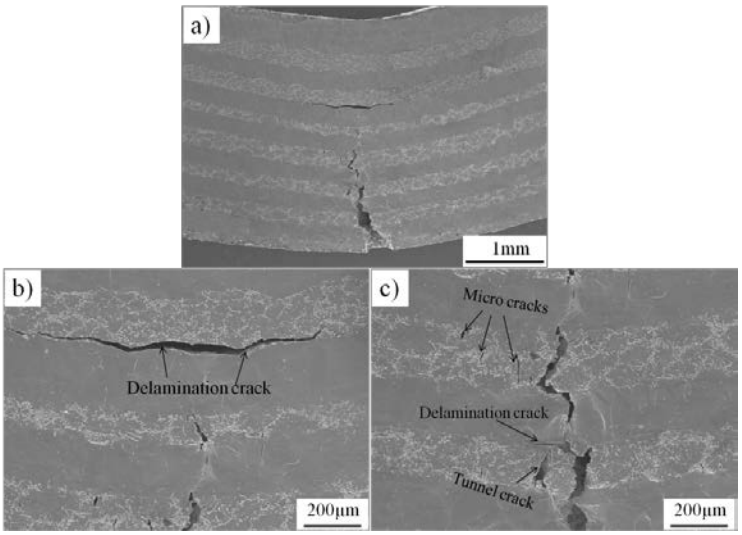

Fig. 3. Three-point bending fractographs of laminated Ti-(TiBw/Ti) composites fabricated at 1100ºC. a) a low magnification; b) and c) a high magnification.

Fig. 4 shows the bending fracture characteristics of laminated Ti-(TiBw/Ti) composites fabricated at 1000ºC and 1200ºC, respectively. Fig. 4a illustrates many delamination cracks initiated by weak interfaces. There are no obvious plastic deformation traces appeared in Ti layer, which is related to low deformation capacity. Based on classical bending theory, serious delamination behavior can sharply result into the increase of bending normal stress, this chain phenomenon may lead to early rupture of laminated Ti-(TiBw/Ti) composites. While tortuous main crack propagation trace without delamination crack is appeared in the laminated composites fabricated at 1200ºC as shown in Fig. 4b), the strong interface prevent the formation of interfacial delamination crack. Therefore, the laminated Ti-(TiBw/Ti) composites fabricated at 1200ºC displays sharply fracture stage when the load reaches to peak value, which is attributed to the absence of delamination crack.

The bending fracture characteristics depicted by schematic diagram is shown in Fig. 5. The deformation curvature radius (ρ) of beam is associated with an applied load F during three-point bending process. There is a neutral line with constant length existing in the middle of beam as shown in Fig. 5a), above which the length of beam is shorten, while below which the length is elongated as shown in Fig. 5b). Therefore, supposing the strain in the beam begins varying linearly along its thickness in a cone shape, and above the neutral line the stress state is compressive, while below the neutral line the stress state is tensile as shown in Fig. 5c). As a matter of fact, the composites failure is associated with tensile stress during bending test [16]. Therefore, the tensile strain ε and tensile stress σ under the neutral line could be simply expressed by the following equations:

$$\varepsilon = \frac{(\rho + y)d\theta - \rho d\theta}{\rho d\theta} = \frac{y}{\rho} \tag{2}$$

$$\sigma = E\varepsilon = E\frac{y}{\rho} \tag{3}$$

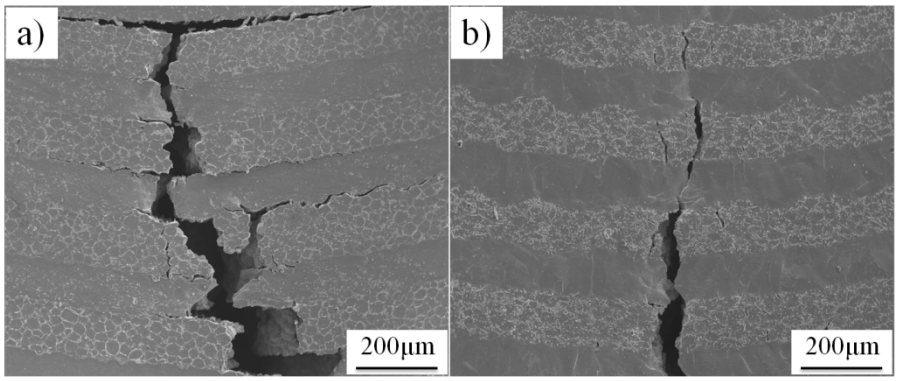

Fig. 4. Bending fractographs of laminated Ti-(TiBw/Ti) composites fabricated at different diffusion welding temperature. a) 1000ºC; b) 1200ºC.

where E is the elastic modulus of Ti layer or TiBw/Ti composite layer, y is the distance to neutral axis. According to the above equation, the tensile strain for bending samples is only related to the location and the curvature radius. However, the tensile stress distribution in the laminated Ti-(TiBw/Ti) composites is a piecewise linear distribution along bending direction as shown in Fig. 5c), which is attributed to the different elastic modulus of Ti layer and TiBw/Ti composite layer. Hence TiBw/Ti composite layer suffer from high stress while Ti layer suffer low stress. With the increase of tensile strain and stress, the generation of tunnel cracks is appeared in the TiBw/Ti composite layer, which are initiated by nucleation, growth and coalescence of micro-cracks.

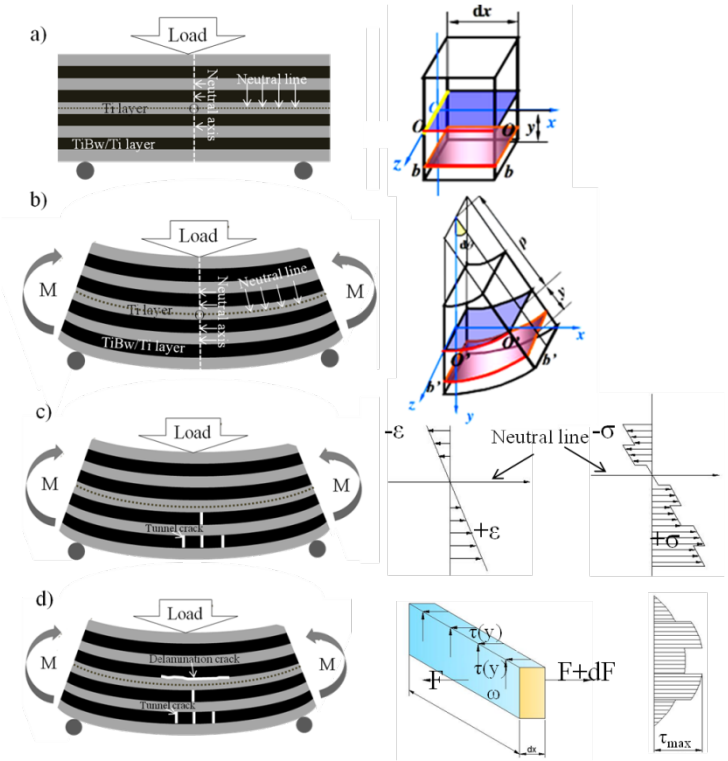

Fig. 5. a)-d) Schematic diagram of bending fracture characteristics and stress distribution of laminated Ti-(TiBw/Ti) composites.

Moreover, expect for normal stress, there is a shear stresses distribution along the bending direction of laminated Ti-(TiBw/Ti) composites. There is force equilibrium on the composites as follows [17, 18]:

$$F + \tau(y) b dx = F + dF \tag{4}$$

$$F = \int_{\omega} \sigma dA \tag{5}$$

$$\tau_{\max} = \frac{3}{2}\frac{F_s}{A} \tag{6}$$

Fig. 5d) shows the bending shear stress of laminated Ti-(TiBwTi) composites, and the maximum shear stress occurs at the neutral line, the delamination crack is initiated by the shear stress during bending process. In general, shear stress should be neglected due to that it is far below the tensile stress. However, the shear stress must be considered for laminated Ti-(TiBw/Ti) composites with weak interfacial bonding strength.

An increased load accompanying with the increase of curvature radius gives rise to the formation of more tunnel cracks in the TiBw/Ti composite layer, and the stress intensity factor (K_I) of fracture mode I was obtained by introducing the tip of tunnel crack. The following expressions from linear elastic fracture mechanics (LEFM) were used for the stress around the tunnel crack tip under the plane stress condition [19].

$$\sigma_x = \frac{K_I}{\sqrt{2\pi r}}\cos\frac{\theta}{2}\left(1-\sin\frac{\theta}{2}\sin\frac{3\theta}{2}\right) \tag{7}$$

$$\sigma_y = \frac{K_I}{\sqrt{2\pi r}}\cos\frac{\theta}{2}\left(1+\sin\frac{\theta}{2}\sin\frac{3\theta}{2}\right) \tag{8}$$

$$\tau_{xy} = \frac{K_I}{\sqrt{2\pi r}}\sin\frac{\theta}{2}\cos\frac{\theta}{2}\cos\frac{3\theta}{2} \tag{9}$$

$$K_I = \sigma\sqrt{\pi a} \tag{10}$$

It is obvious that the local stresses could rise to extremely high level as distance (r) approaches zero. However, there is a region of plastic deformation zone developed near the tunnel crack tip, this circumstance is precluded by the onset of plastic deformation at the tunnel crack tip. Consider three principal stress according to mechanics of materials, an estimate of the size of plastic deformation zone under plane stress state should be calculated as follows:

$$\sigma_1 = \frac{\sigma_x+\sigma_y}{2} + \sqrt{\left(\frac{\sigma_x-\sigma_y}{2}\right)^2 + \tau_{xy}^2} \tag{11}$$

$$\sigma_2 = \frac{\sigma_x+\sigma_y}{2} - \sqrt{\left(\frac{\sigma_x-\sigma_y}{2}\right)^2 + \tau_{xy}^2} \tag{12}$$

$$\sigma_3 = 0 \tag{13}$$

The elastic stresses existing directly ahead of the crack will be fitting to the Mises yield criterion, and the size of plastic zone is expressed [20]:

$$\left(\sigma_1-\sigma_2\right)^2+\left(\sigma_2-\sigma_3\right)^2+\left(\sigma_1-\sigma_3\right)^2 = 2\sigma_s^2 \tag{14}$$

$$r_y = \frac{K_I^2}{2\pi\sigma_s^2}\cos^2\frac{\theta}{2}\left(1+3\sin^2\frac{\theta}{2}\right) \tag{15}$$

$$r_y = \frac{K_I^2}{2\pi\sigma_s^2}\cos^2\frac{\theta}{2}\left(1+3\sin^2\frac{\theta}{2}\right)\ (\theta=0) \tag{16}$$

Since the presence of the plastic zone makes the tunnel crack slightly longer than actually measured, the apparent crack length is assumed to be the actual crack length plus plastic zone size as a result of load redistribution around the zone, and the apparent stress intensity factor is expressed as follows:

$$K_{apparent} = \sigma\sqrt{\pi\left(a+\frac{1}{2\pi}\frac{K_{apparent}^2}{\sigma_s^2}\right)} \tag{17}$$

Since the plastic zone size is itself dependent on the stress intensity factor, the value of $K_{apparent}$ must be determined:

(18)

$$K_{apparent}=\frac{\sigma\sqrt{\pi a}}{\left[1-\frac{1}{2}\left(\frac{\sigma}{\sigma_S}\right)^2\right]^{\frac{1}{2}}}$$

Therefore, there are obvious localized plastic deformation traces and slight delamination cracks existed at the tunnel crack tip, which is the same as the plastic zone shape. The apparent stress intensity factor will give rise to fracture toughness (K_{IC}) with the increase of tensile normal stress, inducing the shear fracture of pure Ti layer.

4 CONCLUSIONS

(1) Three kinds of laminated Ti-(TiBw/Ti) composites were successfully fabricated at different diffusion welding temperatures of 1000ºC, 1100ºC and 1200ºC. The relative interfacial pores and delamination cracks are decreased with increasing the diffusion welding temperature;

(2) The laminated Ti-(TiBw/Ti) composites fabricated at 1100ºC reveal the highest bending ductility and bending toughness, which is attributed to the moderate interfacial bonding strength;

(3) During the bending testing, the formation of tunnel crack may be related to the high tensile strain and stress in the TiBw/Ti composite layer, while delamination crack may be initiated by shear stress.

ACKNOWLEDGEMENTS

This work is financially supported by the National Natural Science Foundation of China (NSFC) under Grant Nos. 51601055 and 51401068, the National Natural Science Foundation of Hebei Province under Grant Nos. E201620218, QN2016029, China Postdoctoral Science Foundation Funded Project (Grant no. 2013M541370), Heilongjiang Postdoctoral Fund (Grant no. LBH–Z13098) and Fundamental Research Funds for the Central Universities (Grant No. HIT.BRETIII.201401 and 2014001).

REFERENCES

[1] S.C. Tjong, Y.W. Mai. Processing-structure-propertiy aspects of particulate- and whisker-reinforced titanium matrix composites. Compos. Sci. Technol. 68 (2008) 583-601.
[2] J.H. Wang, X.L. Guo, J.N. Qin, D. Zhang, W.J. Lu. Microstructure and mechanical properties of investment casted titanium matrix composites with B_4C additions. Mater. Sci. Eng. A. 628 (2015) 366-373.
[3] X. Guo, L. Wang, M. Wang, J. Qin, D. Zhang, W. Lu, Metall. Mater. Trans. A 43 (2012) 3257–3263.
[4] K. Lu. The future of metals. Science. 328 (2010) 319-320.
[5] K. Lu. Making strong nanomaterials ductile with gradients. Science. 345 (2014) 1455-1456.
[6] L.J. Huang, L. Geng, H.X. Peng. Microstructurally inhomogeneous composites: is a homogeneous reinforcement distribution optimal? Progress in Materials Science. 71 (2015) 93-168.
[7] Y. Kimura, T. Inoue, F.X. Yin, K. Tsuzaki. Inverse temperature dependence of toughness in an ultrafine grain-structure steel. Science. 320 (2008) 1057-1060.
[8] T.H. Fang, W.L. Li, N.R. Tao, K. Lu. Revealing extraordinary intrinsic tensile plasticity in gradient nano-grained copper. Science 331 (2011) 1587-1590.
[9] M.J. Liu, Z. Wang, J.Y. Wu, Q.G. Li, C. Wu, Y.Y. Li. Effects of Nb on the elements diffusion and mechanical properties of laminated Ti/Al2O3 composites. Mater. Sci. Eng. A. 636 (2015)

263-268.
[10] W. J. Clegg, K. Kendall, N. Mcn. Alford, T. W. Button & J. D. Birchall. A simple way to make tough ceramics. Nature 1990; 347: 455-457.
[11] L. Jiang, Z. Q. Li, G.L. Fan, L.L. Cao, D. Zhang. The use of flake powder metallurgy to produce carbon nanotube (CNT)/aluminum composites with a homogenous CNT distribution. Carbon 2012; 50: 1993-1998.
[12] B.X. Liu, L.J. Huang, L. Geng, B. Wang, X.P. Cui. Effects of reinforcement volume fraction on tensile behaviors of laminated Ti-TiBw/Ti composites. Mat. Sci. Eng. A. 610 (2014) 344-349.
[13] B.X. Liu, L.J. Huang, L. Geng, B. Wang, X.P. Cui. Fracture behaviors and microstructural failure mechanisms of laminated Ti-TiBw/Ti composites. Mat. Sci. Eng. A. 611 (2014) 290-297.
[14] B.X. Liu, L.J. Huang, B. Wang, L. Geng. Effect of pure Ti thickness on the tensile behavior of laminated Ti-TiBw/Ti composites. Mat. Sci. Eng. A. 617 (2014) 115-120.
[15] B.X. Liu, L.J. Huang, L. Geng, B. Wang, C. Liu, W.C. Zhang. Fabrication and superior ductility of laminated Ti-TiBw/Ti composites. Journal of Alloys and Compounds. 602 (2014) 187-192.
[16] Y.B. Sun, J. Chen, F.M. Ma, K. Ameyama, W.L. Xiao, C.L. Ma. Tensile and flexural properties of multilayered metal/intermetallics composites. Mater. Charact. 102(2015) 165-172.
[17] B.H. Jiang, Z.B. Li, F.Y. Lu. Failure mechanism of sandwich beams subjected to three-point bending. Compos. Struct. 133 (2015) 739-745.
[18] H. Yoshihara. Interlaminar shear strength of medium-density fiberboard obtained from asymmetrical four-point bending tests. Constr. Build. Mater. 34 (2012) 11-15.
[19] P. Agrawal, C.T. Sun. Fracture in metal-ceramic composites. Compos. Sci. Technol. 64 (2004) 1167-1178.
[20] K.J. Hsia, Z. Suo, W. Yang. Cleavage due to dislocation confinement in layered materials. J. Mech. Phys. Solids. 42 (1994) 877-896.